WORLD CONFERENCE ON TIMBER ENGINEERING 2025
BRISBANE, AUSTRALIA

Advancing Timber for the Future Built Environment

Fiber structures and tensile out-of-interface properties of natural *Ficus* inosculated connections

Xiuli Wang[1], Robert Koller[1], Jan-Willem van de Kuilen[2]

ABSTRACT: Trees can adapt to external loads and form inosculated connections (i.e., self-growing connections). During this process, the connection can optimize its shape and internal fiber morphology to fulfill its physiological and mechanical functions. This self-optimization can inspire nature-based design, but requires a deeper understanding of fiber features and the resulting mechanical strength of a connection. This paper focused on living tree connections fused by *Ficus benjamina* L. To describe connections' growth stages, the interface curvature was proposed and measured. Fiber structures were characterized by optical microscopy. Tensile-out-of-interface tests were designed and conducted to measure the tensile strength and maximum resistance. Curved merged fibers at the interface provided primarily bonding strength and structural integrity to a connection. Tensile strength ranged from 0.29 to 1.30 MPa, depending on the growth stage of a connection. The interface curvature of a connection was found to be negatively correlated with its strength. Meanwhile, it could distinguish failure modes from failure at the interface to failure across stems at around 60%. The tensile failure of a connection was mainly caused by the combination of rolling shear and perpendicular tension of the merged fibers.

KEYWORDS: adaptive growth, inosculation, building with nature, biomechanics

1 – INTRODUCTION

Wood is a natural material with heterogeneity, anisotropy, and hierarchical structures. These characteristics are the result of the complex growth processes of a tree [1]-[3]. Trees can sense external forces, such as wind, gravity and snow, and respond through adaptive growth, known as thigmomorphogenesis [4]-[7]. During the adaptive process, the cross-sectional shapes, density, and internal fiber orientation are optimized to efficiently distribute biomass [8], [9]. This structural optimization helps to enhance the mechanical resilience and stability of trees, which offers inspiration for material design [10] and structural engineering [11].

The formation of inosculations (i.e., self-growing connections in this research) is based on the mechanism of adaptive growth and the grafting of trees [12]. As illustrated in Figs. 1a and b, when two trees are constrained at their contact interface, in response to compressive stresses, the contact interface develops a shared cambium layer through the division of callus tissues. Over time, this process gradually fuses two trees into a stable and unified connection. Studies have shown that root grafting may enhance trees' survival capacity and bring ecological benefits [13]. Similarly, fusing tree stems into an itegrated bracing system may further improve the stability of individual trees to resist wind loads [11], [14]. As shown in Fig. 1c, a braided net structure can be created using living connections. As a result, this allows them to reinforce the planar stiffness, and thus to better withstand external loads. However, to the best knowledge of the authors, the growth characteristics and mechanical properties of naturally formed connections remain underexplored.

Optimization of fiber structures plays a critical role, particularly at the interface between stems and branches. With regard to the self-growing connection formed by stems, the interface shapes like a saddle on a three dimensional surface as in Figs. 1d and e. Compared to

[1] Xiuli Wang, Institute of Bio- and Geosciences, IBG-2: Plant Sciences, Forschungszentrum Jülich GmbH, Jülich, Germany, xiu.wang@fz-juelich.de

[1] Robert Koller, Institute of Bio- and Geosciences, IBG-2: Plant Sciences, Forschungszentrum Jülich GmbH, Jülich, Germany, r.koller@fz-juelich.de

[2] Jan-Willem van de Kuilen, Wood Technology, Department of Materials Engineering, Technical University of Munich, Munich, Germany, vandekuilen@hfm.tum.de

https://doi.org/10.52202/080513-0663

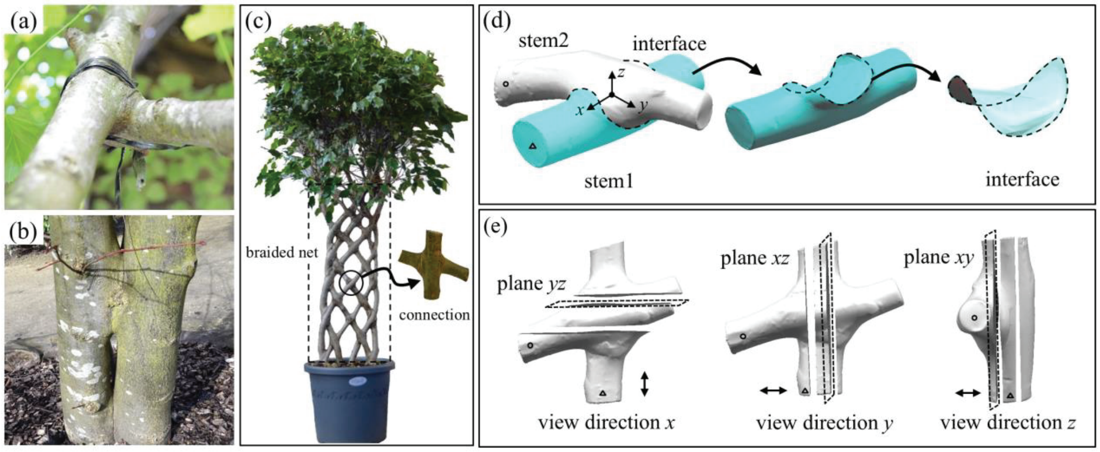

Figure 1 Self-growing connections and its constructed structures. (a) Cross and (b) parallel connections fused by *Tilia* trees; (c) A braided net formed by *Ficus* trees and connections; (d) The interface of a connection between two stems. (e) Three view directions according to the coordinates defined in (d).

stem-branch connections, studies [15], [16] show that the fiber structure exhibits an interlocked fiber pattern. This structural optimization helps improve strength and improve fracture toughness [17]. Similarly, regarding the self-growing connection, its fiber structure at the interface and the corresponding mechanical strength determine its structural potential. Given that the strength in the transverse direction is an order of magnitude lower than in the longitudinal direction, the resistance of a connection to its splitting of the interface presents a potential weak scenario. Consequently, the mechanical behavior of the interface under tension is the key focus of this study.

Measuring the mechanical performance of self-growing connections during their growth presents several challenges. First, the formation and growth rate of a connection is influenced by the species and its growing conditions. Many tree species can fuse connections, such as lime [11], willow [18], and *Ficus* [19], among which *Ficus* is a relatively fast-growing species and have feasibility to form connections and fit the timeframe of the research [20], [21]. Second, naturally formed connections often have an irregular shape and size, which requires adaptable equipment to measure and ensure their accuracy. Lastly, quantifying the characteristics of connections at different growth stages and correlating these characteristics with their mechanical strength remains a challenge.

This study uses connections with different growth stages formed by *Ficus* trees. The purpose of this project is to characterize the structure of the wood fibers and analyze mechanical strength [14], [22], [23]. In engineering design, wooden structures predominantly utilize tree trunks, while branches and curved stems are often considered waste. Investigating the mechanical and ecological value of these naturally grown structures not only promotes efficient resource utilization but also offers insights for sustainable design.

2 – Materials and methods

2.1 Self-growing *Ficus* connections

This research investigated the biomechanics of self-growing connections formed by *Ficus* trees. Connections were cut from braided tree structures formed in a planar pattern (as shown in Fig. 1c). As listed in Table 1, a total of five braided tree structures were used. Each braided tree structure consisted of six stems braided in pairs, creating self-growing connections at intervals of 50 to 200 mm. All connections were studied in its fresh condition, which means connections were tested immediately after they were cut from the trees. Within the braided tree structures, they provided connections in different growing stages, from the early stage of merging to fully connected as a unity. In total, 84 connections were prepared for the subsequent investigations.

Table 1: Size information about the braided trees for mechanical tests

ID	Diameter (mean±CoV, mm)	Number of tests
Tree A	23.0 ± 15.9%	14
Tree B	20.2 ± 20.7%	16
Tree C	22.2 ± 12.5%	18
Tree D	20.8 ± 8.3%	18
Tree E	17.9 ± 16.2%	18
Total	-	84

2.2 Influencing parameters on out-of-interface tensile properties

https://doi.org/10.52202/080513-0663

To accurately quantify the factors that influence the tensile properties of the *Ficus* connections, several parameters were measured. These included basic density, moisture content, average diameters, and interfacial area of connections. Most importantly, the parameter to quantify growth stages was evaluated, which was defined as the interface curvature.

The basic density was calculated as the ratio of the dry mass (wood mass) to the green volume, as in Equation (1). Given the irregular shape of the connections, the water displacement method was used to measure the volume. A freshly cut connection was inserted into a beaker filled with water. The volume of water displaced by the connection was considered its green volume. The green mass was determined immediately after cutting the connection from the tree. After mechanical tests, connections were dried in an oven until a constant dry wood mass was achieved, in accordance with the EN13183 standard [24].

$$\rho = \frac{M_\mathrm{d}}{V_\mathrm{g}}, \tag{1}$$

where ρ represents the basic density of a connection, in kg/m^3; M_d and V_g denote the dry mass and green volume, respectively.

curved area (A_curved), with a resolution of 1 mm. The outer layer of a connection was obtained from scanning, as shown in Fig. 2b, and subsequently the data were processed using VXElement to create a mesh model from the point-cloud data. The edge of the connected area (Fig. 2c) was manually identified as a cutting curve to separate two stems and expose to the interface. The 3D surface was reconstructed by selecting the nearest three points to generate a mesh with a resolution of no less than 5 mm^2. Consequently, the curved area was formed and measured (Fig. 2d). The mapped plane *xy* was the mechanical loading plane constructed by the center line of one stem with a normal vector perpendicular to the other center line of another stem. The curved interface was then projected to this plane, and the resulting planar surface was measured as the projected area (A_proj). The interface curvature (C) was derived from the ratio of the projected area to the curved area, as expressed in Equation (2).

$$C = \frac{A_\mathrm{proj}}{A_\mathrm{curved}} \times 100\%, \tag{2}$$

It was proposed as a parameter to describe the shape of the interface. Physically, it explained the percentage of the area that a connection can mobilize when resisting an external force.

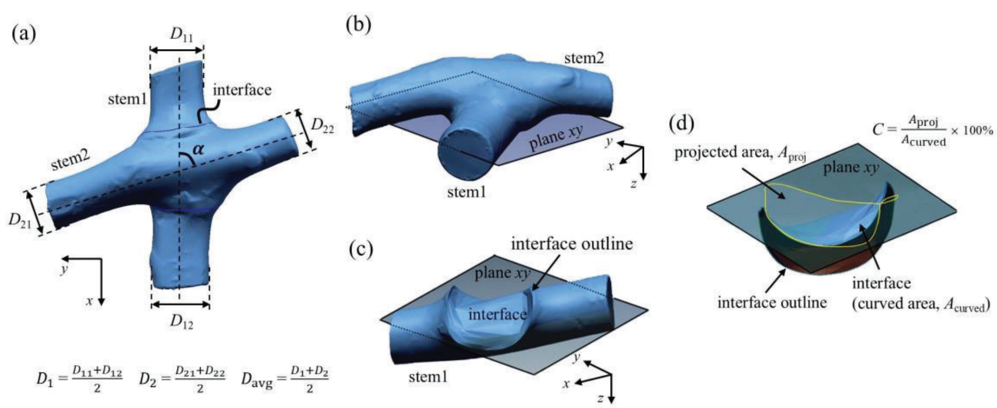

Figure 2 Illustration of the approach to derive the interface curvature of a self-growing connection. (a) Reconstructed model from the surface scanning; (b) Plot of the reference plane, plane *xy*, according to the loading situation; (c) Separation of two stems based on the outline of interface; (d) Projection of the curved interface to the reference plane *xy*, forming a projected area.

The moisture content (MC) was measured by dividing the mass of water in the connection by the dry wood mass. As shown in Fig. 2a, the diameter of the connection is represented by the average of the diameters measured at the four ends. During the preparation of connections, the diameters of the tree stems forming the connections were similar, with a difference of less than 5%. Therefore, the variation in stem diameters was not considered.

To measure the interface, a scanner equipment (HandyScan 3D, Creaform) was utilized to measure the

2.3 Fiber structures

The fiber structure of a connection was observed using an optical microscope (Keyence VHX-3000, Germany). Observations were conducted on three orthogonal viewing directions, as shown in Fig. 1e, to enhance the understanding of the three-dimensional orientation of the fibers within a connection.

2.4 Tensile out-of-interface tests

The tensile out-of-interface setup was designed with adjustable load-transfer clamps, as seen in Fig. 3. Two adjustable rails were fastened to the moving platform at the bottom and connected the load cell at the top, which provided a spatial four-point loading system, as illustrated in Figs. 3b and c. The analysis utilized 3D DIC cameras to gauge the interfacial region, with the ARAMIS (GOM, Germany) program used to assess deformations.

The schematic explanation of the load transfer pathway is presented in Fig. 3d. The tensile forces exerted by the supports (simplified as pins at points A, B, C, and D) were primarily transferred to shear forces on the interface of a connection. The distances L_{AB} and L_{CD} represented the load spans in two stems. These loading spans, excluding the interface width, were limited to twice the diameter size. The average ratio of span to diameter on each side of the stem is 0.88 with a CoV of 47%. This ensured that the forces conveyed to the interface were effectively treated as tensile forces acting on it. Controlled by a bottom loading platform, tensile testing was performed by applying displacements. The platform moved at a constant velocity of 0.02 mm/s. During testing, the upper clamp (located at A and B) remained immobile. The deformations of the connection were quantified by averaging the displacements at the loading points C and D.

Regarding the calculation of the strength of a connection, it is assumed that tensile forces distribute uniformly over the projected area of a connection. The tensile strength of a connection is thus considered as an effective strength over the resistive plane and is calculated by the ratio between the maximum force and its projected area. Calculations of mechanical properties are expressed in Equation (3).

$$f = \frac{F_{\mathrm{m}}}{A_{\mathrm{proj}}}, \quad (3)$$

where f denotes the strength of a connection, in MPa; F_{m} refers to the maximum force from the loading curve, and A_{proj} means the projected area of the connection.

3. Results and discussion

3.1 Fiber structures

Regarding fiber structures of self-growing connections, three major observations can be identified. First, fiber bundles that construct a self-growing connection can be categorized into three groups based on their spatial positions, namely original fibers, deviated fibers, and merged fibers (see Fig. 4a). The group of original fiber bundles formed independently in each stem without any influence of fusion activity. In contrast, the deviated fibers, while located separately in each stem, were influenced by the fusion activity and resulted in deviation in their directions. The merged fibers connected two stems together and produced at both stems. The change in the fiber orientation of the deviated fibers could be explained by the grain-flow analogy as stated in [25], [26].

Second, merged fibers were crucial for the formation and structural properties of a self-growing connection. The distribution pattern of this group of fibers was predominantly observed in the outer layer of a connection (Fig. 4b). The third observation was that old bark tissues before fusion were identified in Figs. 4c and d. As indicated in [27], the bark included before fusion still existed inside and new wood was produced on top of that after fusion. Moreover, little merged fibers are

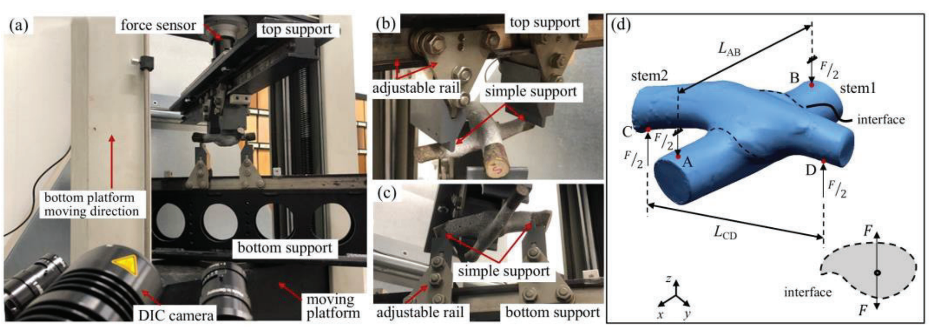

Figure 3 Experimental setup for tensile out-of-interface tests. (a) Overview of the tensile setup with two rotatable clamps, a force sensor, and DIC for measurements; (b) Details of the top clamp which is not movable in vertical direction; (c) Details of the bottom clamp which applies forces to the connection by moving in the z direction; (d) Schematic representation of the tensile load transfer on the connection. The forces (F) are applied through pin support points (A, B, C, and D) within the adjustable distances (L_{AB}, L_{CD}).

https://doi.org/10.52202/080513-0663

found inside a connection compared with the out-layer merged fibers.

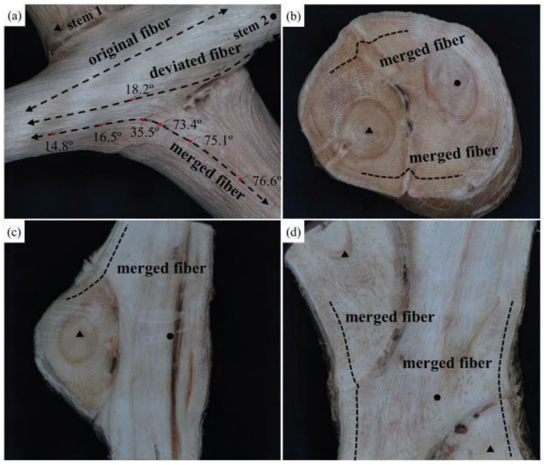

Figure 4 Fiber structures of self-growing connections. (a) Three main fiber groups: merged fiber, deviated fiber, and original fiber. Distributions of merged fibers from the viewing plane of (b) *yz* and (c) *xz* and (d) *xy* according to Fig. 1e.

3.2 Statistical description of influencing parameters

In this study, the measured parameters influencing the tensile properties of connections include density, average diameter, projected area, and interfacial curvature. The tensile out-of-interface properties are characterized by tensile strength and load-bearing capacity. The distributions of these parameters are shown in Fig. 5.

During testing, all connections were maintained in a fresh state with a moisture content of 182.3% ± 6.8%. This moisture content was significantly higher than the fiber saturation point of the wood. Beyond this threshold, it is generally assumed that further increases in moisture content have a negligible impact on the mechanical properties of wood. Therefore, it can be inferred that the moisture content does not significantly interfere with the mechanical results.

The morphology of the connections tested ranged from conditions where two stems were just connected in the bark to conditions where two centerlines of two stems were nearly in a plane. In the first case, the interface curvature can be considered to converge to 100% as the curved interface is nearly flat. In contrast, in the second case, when the two stems completely interlocked, e.g., with a 90° cross angle, the interface curvature converges to around 30% when piths of stems overlapped. Practically during the fusion process, if the tree stems fuse at a diameter of 2 mm and grow to a diameter of 20 mm, when a complete and sound fusion and co-growth is considered, the fusion degree converges to approximately 80%. This analysis attempts to point out that the ranges of growth parameters and mechanical properties are related to all growth levels. In other words, these ranges represent the developmental process of a connection in the course of its growth.

In the measured connections, assuming that the analysis covered the full range of growth, it can be argued that the strength interval of a connection ranged approximately from the strength of the soft tissues to the strength approximate to the wood fibers, from 0.29 to 1.30 MPa. The mean specific density of the connections studied was 0.325 g/cm^3 with a CoV of 12%. Limited research has been conducted on the strength of *Ficus* wood; therefore, reference is made to species with a specific density between 0.3 and 0.36 g/cm^3, such as spruce, fir, and cedar, which have tensile strengths perpendicular to the grain of 1.5, 1.2, and 1.9 MPa, respectively [28]. It can be estimated that the strength of

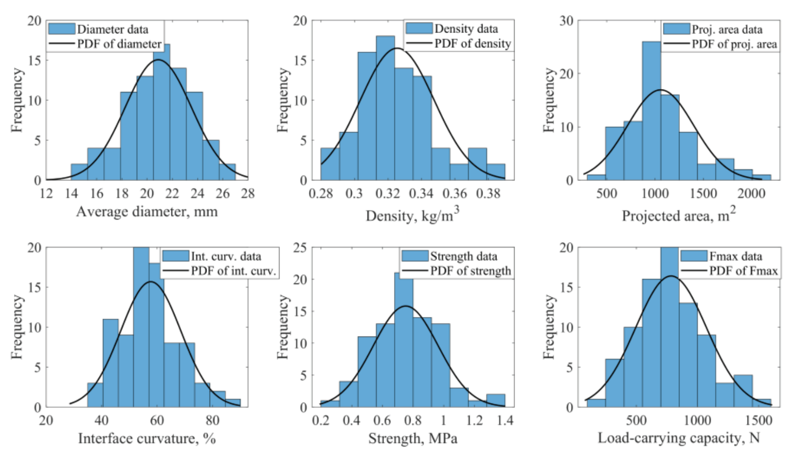

Figure 5 Statistical distributions of measured parameters. (a) Average diameter, (b) density, (c) projected area, (d) interface curvature, (e) tensile strength, and (f) load-carring capacity.

the connection converges to the transverse tensile strength of the wood itself.

3.3 Failure modes and mechanisms

The difference in their failure was mainly attributed to their growth levels. In other words, the failure was mainly influenced by the morphology of the merged fibers. From the results, two failure modes were distinguished: failure at the interface (FM I, Fig. 6a) and failure across stems (FM II, Fig. 6b).

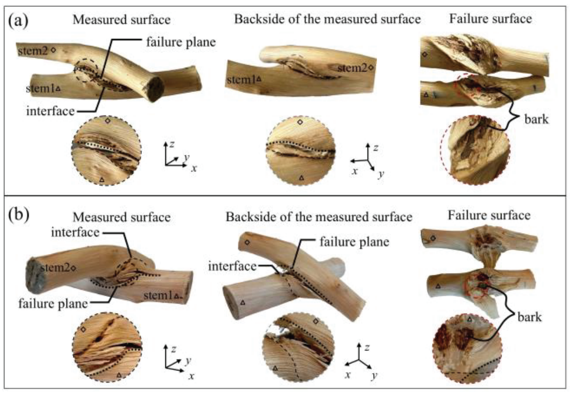

Figure 7 Failure modes of connections after tensile out-of-interface tests. (a) Failure mode I (FM I), the fracture surface occurred at the interface; (b) failure mode II (FM II), the fracture surface occurred at partial the interface and partial within stems.

In failure mode I (Fig. 6a), the cracking surface overlapped the interface. Although a small number of merged fibers were found within the connection, they failed to form an effective bond between the two stems. In contrast, in failure mode II (Fig. 6b), the failure surface only partially overlapped the interface. Connections that failed in FM II had more merged fibers and formed a more curved interface. Cracks first occurred at the corners and then extended along the interface. However, when the crack extension encountered the merged fibers, the crack path no longer followed the interface, but instead followed the direction of the wood grain.

When comparing the strengths in the two failure modes, the strength in failure mode II was slightly higher than that in failure mode I (Fig. 7a). Through t-tests, the result showed the strength difference in two failure modes was significant ($p = 0.002 < 0.05$). The failure modes of connections were closely related to their growth stages and interface curvature. As shown in Fig. 7b, failure mode I and failure mode II can be distinguished at an approximate interface curvature threshold of 60%. When the interface curvature exceeds 60%, cracking surface is more likely to occur entirely at the interface. In contrast, when the curvature is below this threshold, the cracking surface tends to occur partially at the interface and partially within the tree stem. On the basis of previous analyses, as the connection matures, the interface curvature decreases. This corresponds to an increase in mechanical strength, and the failure mode II becomes more predominant.

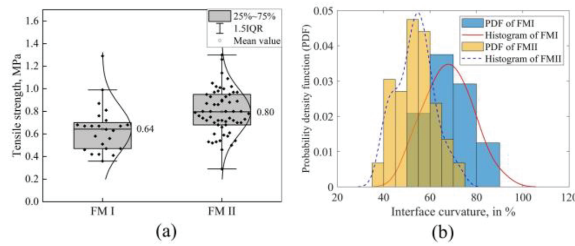

Figure 6 Comparison between failure modes. (a) Comparison of tensile strength between failure modes; (b) Distinguishment of failure modes by the interface curvature.

To measure the strength of a connection, it assumed that the loading forces were uniformly transmitted to the effective interface perpendicular to the loading direction. However, the stress environment at the interface is complex and involves the interaction of shear and tensile stresses. The fiber orientation varies significantly at different positions along the interface [22], as shown at points P_1, P_2, and P_3 in Fig. 8. When applying a tensile force F, the corner at P_1, which lacks continuous fibers, relies mainly on the bark tissue to bear the tensile stress (Figs. 8b and c). In contrast, at point P_2, the tensile stress can be understood as a resultant of perpendicular tensile and shear stresses (Figs. 8 d and e) along the direction of local fibers. The materials in P_3 experience a similar stress environment, but the orientation of the fiber differs from P_2 (Figs. 8 d and f). Therefore, the failure strength of the interface is a combination of the limits of the tensile perpendicular (stress $\sigma_{t,90}$, strength $f_{t,90}$) and shear strength (stress σ_v, strength f_v). The failure criteria can be expressed in Equation (4).

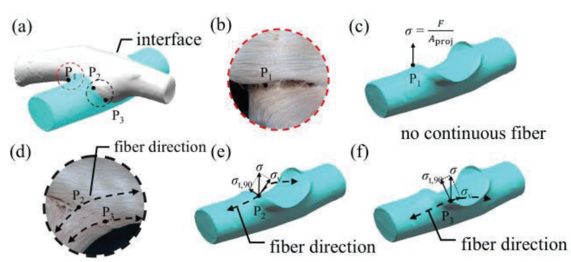

Figure 8 Illustration of the stress and fiber orientation at different points along the interface. (a) Overview of points P_1, P_2, and P_3 at the interface; (b) Fiber morphology of the area in a red circle in (a); (c)At point P_1, no continuous fiber resists tensile stress (σ). (d) Fiber orientations at points P_2 and P_3; area in the black circle is zoomed in (a). (e) Stress components at P2, indicating the interaction of perpendicular tensile stress ($\sigma_{t,90}$), and shear stress (σ_v). (f) Stress components at P_3 according to the direction of the local fiber.

 https://doi.org/10.52202/080513-0663

$$\left(\frac{\sigma_{t,90}}{f_{t,90}}\right)^2 + \left(\frac{\sigma_v}{f_v}\right)^2 \leq 1, \tag{4}$$

To compare the failure plane with the interface and the merged fiber direction in Figs. 8 b and Fig. 7, it was argued that the failure occurred mainly due to a combination of the tensile strength limit of soft tissues, the shear strength limit, as well as the tensile strength limit perpendicular to the wood grain.

3.4 Correlation between influencing parameters and tensile properties

A correlation analysis was conducted between density, diameter, projected area, interface curvature, and the tensile properties of cconnections (tensile strength and load-bearing capacity). As shown in Fig. 9, the results indicated that density had a negligible impact on all parameters. The diameter of a connection showed a strong positive correlation with tensile strength (r = 0.74) and projected area (r = 0.61), while interface curvature was negatively correlated with tensile strength (r = -0.58).

For predicting the strength of a connection, the combination of diameter and interface curvature might be effective. However, there are numerous factors that influence the strength remain difficult to quantify. For example, the amount of merged fibers and the angles of their structural arrangement are not fully captured by current measurements. Furthermore, the randomness of fiber growth and its dependence on environmental conditions (e.g., light and nutrient availability) add to the complexity of the analysis. These challenges underscore the need for more comprehensive methods to better understand the factors that affect the strength of a connection.

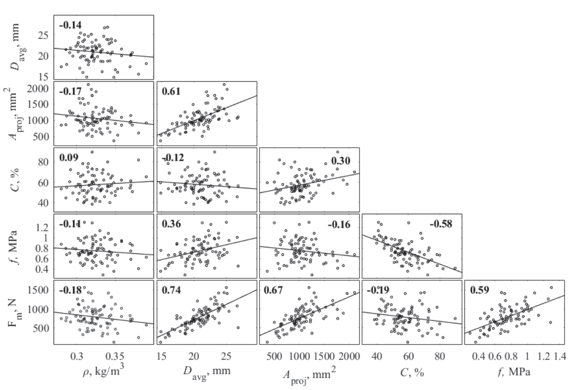

Figure 9 Correlation matrix among parameters, density (ρ), average diameter (D_{avg}), projected area (A_{proj}), interface curvature (C), tensile strength (f), and load-carrying capacity (F_m).

4. Concluding remarks

This study investigated the biomechanical characteristics of *Ficus* connections in various stages of fusion. The analysis focused on the structural morphology of the fibers in the connections and the corresponding tensile strength and load-bearing capacity. The findings are summarized as follows.

- The curved merged fibers are critical for the formation of a connection. These fibers connect the two stems, which ensures the structural integrity and strength of a connection.
- The tensile strength of a connection increases with the degree of fusion, ranging from 0.29 MPa at the initial stage (bark contact) to 1.3 MPa at full fusion.
- The growth level of a connection, as measured by interface curvature, exhibits a negative correlation with the tensile strength. The interface curvature also helps distinguish failure modes into failure at the interface and failure across stems at the threshold of approximately 60%.
- The tensile strength of a connection can be predicted using a combination of the diameter and interface curvature as key parameters.

5. Outlook

Beyond *Ficus* trees, future studies could analyze fusion connections in other tree species to expand the scope of the research. Additionally, mechanical analysis could include shear performance.

In the context of using wood as a building material, curved stems and tree connections are often discarded as waste. By understanding their structural morphology and potential usability, these natural structures could help conserve resources and provide new approaches to sustainable construction.

The adaptive growth of trees is an anisotropic optimization that minimizes material usage while fulfilling multifunctional requirements. Although directly using naturally optimized plant materials involves a long growth cycle, integrating the optimized structures of plants with engineering designs, such as additive manufacturing (3D printing), could offer efficient and innovative solutions.

In forest management, naturally fused connections could be used to form support systems among trees to enhance wind resistance. This provides a natural and sustainable approach to mitigating wind damage in forests.

References

[1] P. Fratzl and R. Weinkamer. “Nature’s hierarchical materials.” In: Progress in materials science 52.8 (2007), pp. 1263–1334.

[2] I. Burgert. “Exploring the micromechanical design of plant cell walls.” In: American journal of botany 93.10 (2006), pp. 1391–1401.

[3] T. Speck and I. Burgert. “Plant stems: Functional design and mechanics.” In: Annual review of materials research 41 (2011), pp. 169–193.

[4] F. W. Telewski and M. J. Jaffe. “Thigmomorphogenesis: Field and laboratory studies of *Abies fraseri* in response to wind or mechanical perturbation.” In: Physiologia plantarum 66.2 (1986), pp. 211–218.

[5] C. Mattheck. “Wood-the internal optimization of trees.” In: Arboricultural journal 19.2 (1995), pp. 97–110.

[6] B. Moulia, S. Douady, and O. Hamant. “Fluctuations shape plants through proprioception.” In: Science 372.6540 (2021), p. eabc6868.

[7] O. Hamant et al. “Developmental patterning by mechanical signals in *Arabidopsis*.” In: Science 322.5908 (2008), pp. 1650-1655.

[8] O. Hamant, J. Traas, and A. Boudaoud. “Regulation of shape and patterning in plant development.” In: Current opinion in genetics & development 20.4 (2010), pp. 454–459.

[9] C. Coutand and B. Moulia. “Biomechanical study of the effect of a controlled bending on tomato stem elongation: local strain sensing and spatial integration of the signal.” In: Journal of experimental botany 51.352 (2000), pp. 1825–1842.

[10] C. Houriet, B. Ulyanov, J. A. Pascoe, and K. Masania. “Wood-inspired interlocking junctions using 3D-printed liquid crystal polymers.” In: Additive manufacturing 97 (2025), p. 104590.

[11] X. Wang, W. Gard, H. Borska, B. Ursem, and J. W. G. van de Kuilen. “Vertical greenery systems: from plants to trees with self-growing interconnections.” In: European journal of wood and wood product 78.5 (2020), pp. 1031–1043.

[12] C. W. Melnyk and E. M. Meyerowitz. “Plant grafting.” In: Current biology 25.5 (2015), pp. R183–R188.

[13] E. Stachew, T. Houette, and P. Gruber. “Root systems research for bioinspired resilient design: A concept framework for foundation and coastal engineering.” In: Frontiers in robotics and AI 8 (2021), p. 548444.

[14] X. Wang, W. Gard, Y. Mosleh, and J.W.G. van de Kuilen. “Morphological analysis of inosculated connections in weeping figs: Insights on density, geometry, fiber structures, and compositional variations.” In: Wood science and technology 59.1 (2025), pp. 1-21.

[15] D. Slater and A. R. Ennos. “Determining the mechanical properties of hazel forks by testing their component parts.” In: Trees – structure and function 27.6 (2013), pp. 1515–1524.

[16] D. Slater and A. R. Ennos. “Interlocking wood grain patterns provide improved wood strength properties in forks of hazel (*Corylus avellana* L.).” In: Arboricultural journal 37.1 (2015), pp. 21–32.

[17] S. Özden, D. Slater, and A. R. Ennos. “Fracture properties of green wood formed within the forks of hazel (*Corylus avellana* L.).” In: Trees – structure and function 31.3 (2017), pp. 903–917.

[18] F. Ludwig, H. Schwertfreger, and O. Storz. “Living systems: designing growth in Baubotanik.” In: Architectural design 82.2 (2012), pp. 82–87.

[19] F. Ludwig, W. Middleton, F. Gallenmüller, P. Rogers, and T. Speck. “Living bridges using aerial roots of *Ficus elastica* – an interdisciplinary perspective.” In: Scientific report 9.1 (2019), p. 12226.

[20] M. H. Zimmermann, A. B. Wardrop, and P. B. Tomlinson. “Tension wood in aerial roots of *Ficus benjamina* L.” In: Wood science and technology 2.2 (1968), pp. 95–104.

[21] E. J. Veneklaas, M. P. R. M. Santos Silva, and F. Den Ouden. “Determinants of growth rate in *Ficus benjamina* L. compared to related faster-growing woody and herbaceous species.” In: Scientia Horticulturae 93.1 (2002), pp. 75–84.

[22] X. Wang. “Build with Nature: Biomechanical properties and performance of self-growing connections in interconnected trees.” PhD thesis. Technology University of Delft, 2024.

[23] X. Wang, W. Gard, and J. W. van de Kuilen. “Biomechanical analysis of inosculations (self-growing connections) in *Ficus benjamina* L.: Impact of

https://doi.org/10.52202/080513-0663

developmental growth levels on mechanical properties.” In: Construction and building materials 462 (2025), p. 139672.

[24] EU Standization. “EN13183-1: Moisture content of a piece of sawn timber - Part 1: Determination by oven dry method.” 2002.

[25] C. Foley. “A three-dimensional paradigm of fiber orientation in timber.” In: Wood science and technology 35.5 (2001), pp. 453–465.

[26] E. M. Kramer. “Wood grain pattern formation: A brief review.” In: Journal of plant growth regulation 25.4 (2006), pp. 290–301.

[27] D. C. Trinh et al. “How mechanical forces shape plant organs.” In: Current biology 31.3 (2021), pp. R143–R159.

[28] D. Kretschmann. “Chapter 5 Wood as an engineering material.” In: Wood handbook (2010), pp. 1–46.